

Assessing air quality dynamics during short-period social upheaval events in Quito, Ecuador, using a remote sensing framework

César Iván Álvarez, Santiago López, David Vásquez, Dayana Gualotuña

Angaben zur Veröffentlichung / Publication details:

Álvarez, César Iván, Santiago López, David Vásquez, and Dayana Gualotuña. 2024. "Assessing air quality dynamics during short-period social upheaval events in Quito, Ecuador, using a remote sensing framework." Remote Sensing 16 (18): 3436. <https://doi.org/10.3390/rs16183436>.



Article

Assessing Air Quality Dynamics during Short-Period Social Upheaval Events in Quito, Ecuador, Using a Remote Sensing Framework

Cesar Ivan Alvarez ^{1,*} , Santiago López ², David Vásquez ¹ and Dayana Gualotuña ¹

¹ Department of Environmental and Civil Engineering, Environmental Research Group on Sustainable Development (GIADES), Salesian Polytechnic University, Quito 170702, Ecuador; jvasquez2@est.ups.edu.ec (D.V.); dgualotuna@ups.edu.ec (D.G.)

² School of Interdisciplinary Arts and Sciences, University of Washington Bothell, Bothell, WA 98011, USA; cslopez@uw.edu

* Correspondence: calvarezm@ups.edu.ec; Tel.: +593-984647745

Abstract: This study uses a remote sensing approach to investigate air quality fluctuations during two short-period social upheaval events caused by civil protests in 2019 and the COVID-19 pandemic in 2020 in Quito, Ecuador. We used data from the TROPOMI Sentinel-P5 satellite to evaluate the concentrations of two greenhouse gases, namely O₃ and NO₂. TROPOMI Sentinel-P5 satellite data are becoming essential in air quality monitoring, particularly for countries that lack ground-based monitoring systems. For a better approximation of satellite data with ground data, we related the remotely sensed data using ground station data and Pearson correlation analysis, which revealed a significant association between the two sources ($0.43 \leq r \leq 0.78$). Using paired *t*-test comparisons, we evaluated the differences in mean gas concentrations at 30 randomly selected intervals to identify significant changes before and after the events. The results indicate noticeable changes in the two gases over the three analysis periods. O₃ significantly decreased between September and November 2019 and between March and May 2020, while NO₂ significantly increased. NO₂ levels decreased by 18% between February and March 2020 across the study area, as indicated by remote sensing data. The geovisualization of remotely sensed data over these periods supports these patterns, suggesting a potential connection with population density. The results show the complexity of drawing global conclusions about the impact of social disruptions on the atmosphere and emphasize the advantages of using remote sensing as an effective framework to address air quality changes over short periods of time. This study also highlights the advantages of a remote sensing approach to monitor atmospheric conditions in countries with limited air quality monitoring infrastructure and provides a valuable approach for the evaluation of short-term alterations in atmospheric conditions due to social disturbance events.



Citation: Alvarez, C.I.; López, S.; Vásquez, D.; Gualotuña, D. Assessing Air Quality Dynamics during Short-Period Social Upheaval Events in Quito, Ecuador, Using a Remote Sensing Framework. *Remote Sens.* **2024**, *16*, 3436. <https://doi.org/10.3390/rs16183436>

Academic Editors: Dongmei Chen and Yuhong He

Received: 11 August 2024

Revised: 10 September 2024

Accepted: 13 September 2024

Published: 16 September 2024

Keywords: air quality; social upheaval; COVID-19 lockdown; remote sensing; sentinel-5P



Copyright: © 2024 by the authors. Licensee MDPI, Basel, Switzerland. This article is an open access article distributed under the terms and conditions of the Creative Commons Attribution (CC BY) license (<https://creativecommons.org/licenses/by/4.0/>).

1. Introduction

Major disruptions like natural disasters, warfare, terrorism, or epidemics, while devastating for human well-being, offer unique opportunities to study human impacts on the Earth system [1]. These events provide new perspectives on the connection between human activity and global environmental change, mainly when precise and reliable data are gathered before, during, and after major disturbance events. For instance, events like the September 11 attack in 2001 raised concerns about atmospheric air quality. Research showed that urban areas near New York experienced decreased air quality due to increased particulate matter emitted into the atmosphere from collapsed buildings and heightened road traffic after airport shutdowns [2]. More recently, COVID-19 significantly affected urban mobility and air quality, with surveys worldwide indicating a substantial reduction

in road trips and ground traffic in the US, dropping by about 65% [3,4]. Moreover, air transportation plummeted, with flights decreasing by over 89% in the European Union [5] and over 90% in the US compared to pre-pandemic levels. These shifts in mobility led to markedly improved air quality due to lockdown enforcement [6]. However, air quality does not always improve due to restrictions on mobility. Other types of unrest, like civilian protests, often worsen air quality due to the burning of hazardous materials and the increased emission of particulate matter into the atmosphere [7–9]. Civilian protests can also alter mobility patterns and disrupt traffic flow by placing temporary barriers on roads, which may reduce pollution and eventually enhance air quality. Thus, the complex interplay between air quality and social unrest remains poorly understood. Our study aims to improve our understanding of how urban shutdowns and mobility disruptions resulting from major social upheaval events and lockdowns impacted air quality in Quito, Ecuador, a large urban conglomerate in northern South America, historically affected by poor air quality.

Latin America has faced social unrest in recent decades due to worsening socio-economic conditions, notably including a rise in informal economic activities. This trend has hindered economic recovery, particularly during severe recessions caused by global events like the COVID-19 pandemic and market collapses, leading to supply chain disruptions [10]. These economic crises sparked civil protests [11], positively and negatively impacting the environment. For instance, the 2019 protests in Ecuador, Colombia, and Chile involved the burning of various materials, causing air pollution and likely decreasing air quality in urban areas [12], particularly in areas with high population densities, where protests were more severe due to higher socio-economic activity. However, the subsequent halt in urban traffic following the protests likely temporarily improved air quality. In 2022, Ecuador saw further protests due to increased gas prices, reflecting the rising frequency of such events across Latin America. These events affect social dynamics in urban environments and may have a long-term effect on the environmental conditions of the areas where the protests occur [13]. Similarly, various studies like those by [14–16] have explored the effects of COVID-19 lockdowns on air quality using remote sensing technologies and demonstrated the effectiveness of these approaches in capturing emerging air quality conditions caused by sudden changes in social behavior. Our study follows this approach and utilizes satellite data to analyze changes in air pollutants at the city and sub-city district (parish or *parroquia* in Spanish) levels caused by COVID-19 lockdowns and civil protests in Ecuador. By demonstrating the effectiveness of remote sensing in monitoring local air quality and emissions, we emphasize remote sensing's cost-effective advantages over traditional methods that involve expensive monitoring equipment.

Increased pollutant concentrations have well-documented impacts on the Earth's climate and public health. Contemporary climate change is closely linked to heightened levels of air pollutants [17], including CO₂, which directly contribute to rising temperatures and global climate shifts [18]. Human activities, such as urban traffic and industrial operations, have significantly increased the atmospheric concentrations of greenhouse gases, including nitrogen dioxide (NO₂), sulfur dioxide (SO₂), and tropospheric ozone (O₃). Carbon monoxide (CO), while not a greenhouse gas itself, aids in forming O₃ and smog, altering the abundance of methane and CO₂. These emissions pose severe health and environmental risks. Elevated NO₂ levels, for instance, may exacerbate the negative impacts of reduced air quality on respiratory conditions [19] and lead to acid rain through water interactions [18]. Exposure to increased SO₂ concentrations has adverse effects on the respiratory, nervous, and cardiovascular systems, causing various public health concerns [20]. Additionally, evidence suggests that O₃ increases mortality risks from respiratory and cardiovascular problems, particularly in young age groups [21,22]. In Latin America, however, the lack of air quality monitoring stations consistent with local-level analysis may lead to incomplete and less accurate air quality and public health assessments, making it difficult to effectively understand, manage, and mitigate air pollution and its impacts. Environmental monitoring has become increasingly crucial in addressing press-

ing environmental issues, with remote sensing technologies emerging as a cost-effective solution for systematic data collection across large regions [23]. Satellite data, for example, are now used for various purposes, such as tracking weather patterns [24], estimating air quality [25], monitoring microplastics [26], and forecasting socio-environmental outcomes, including public health [27]. Remote sensing plays a particularly pivotal role in Latin America, where access to advanced site-based monitoring technology is limited [28]. In this study, we assess changes in urban air quality in Quito, Ecuador, and their association with social unrest and population density based on readily available remotely sensed and census data.

Within this context, our study aims to answer the following research questions: Did social upheaval events and associated restrictions on urban mobility impact air quality in Quito, Ecuador, between 2019 and 2020? If so, were there significant differences in air quality before and after these events at the city and parish (sub city district) levels? We examined changes in NO_2 and O_3 concentrations before and after the civilian protests in 2019 and the COVID-19 lockdowns in 2020. These gases, with well-identified anthropogenic sources, have been commonly studied to understand the atmospheric impacts of COVID-19-related events [29]. The implications of this study are significant and extend far beyond the immediate study area since it provides a cost-effective methodology that could be replicated in other parts of the world to evaluate the impacts of short-term disruptions in the daily life activities of urban citizens caused by short-term social protests and lockdowns. These situations are common in countries affected by socio-political turmoil, which usually lack networks for long-term air quality monitoring.

2. Study Area

Our study focuses on the city of Quito (Figure 1), located at approximately 0.175608°S , 78.484783°W , and at an average elevation of 2850 m.a.s.l, making it the second-highest capital city in the world.

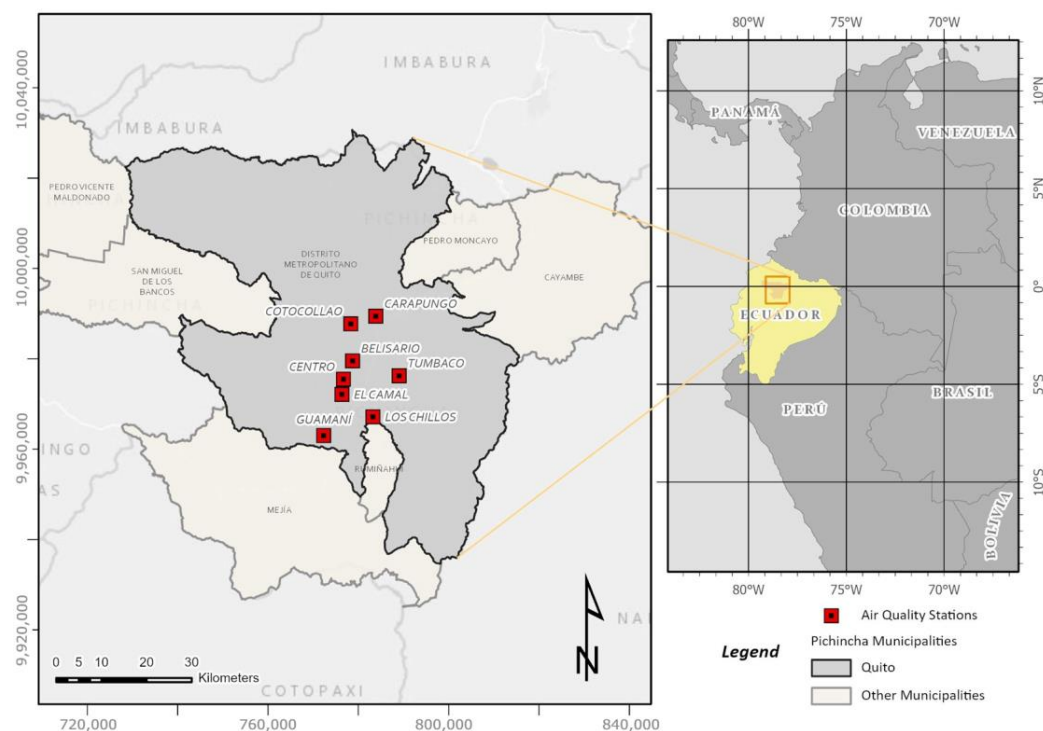


Figure 1. The study area. Quito municipality is depicted in dark grey. Red dots represent air quality ground stations.

The metropolitan district of Quito has a population of about 2.8 million people [30] and is one of the largest urban conglomerates in the Andes. Quito has a relatively constant

and cool climate, with a mean temperature of about 16 °C and a mean annual precipitation of approximately 1000 mm, with an evident influence of the Andean mountains. Although pressure levels vary slightly due to the fluctuations of the intertropical convergence zone (ITCZ), pressure is relatively stable, with rare, very high, or very low-pressure systems occurring throughout the year. Due to its geographic location, Quito receives some of the most significant solar radiation in the world, especially during the drier and clearer-sky months (June–August).

Air quality in Quito is poor due to natural and anthropogenic factors, including air circulation patterns, geomorphology, elevation, increased traffic, the widespread use of old vehicles and machinery, etc. Air quality has experienced a steep decline during the past four decades due to unprecedented unplanned growth. Generally, NO₂ concentrations are usually high and primarily associated with deficient public and private transportation systems that heavily rely on using relatively old vehicles that burn fossil fuels inefficiently, resulting in increased concentrations of greenhouse gases and particulate matter. In addition, with less stringent vehicle emissions regulations and less law enforcement capacity in comparison to developed nations, “dirtier” vehicles freely move across the urban area which negatively impacts air quality, a common characteristic among developing regions [31]. Air quality regulations implemented in the city since the early 2000s led to years of improvement followed by worsening periods, mostly related to increased vehicles and continued use of older automobiles, buses, and trucks. Due to this type of increase and the effects of traffic congestion on productivity (e.g., increased commuting times affecting working hours) and public health, the city of Quito has employed various methods to reduce traffic, improve flow, and improve air quality monitoring. The Metropolitan Network of Atmospheric Monitoring of Quito (REMMAQ), for example, was established in 2003 to monitor air quality and generate data-driven policies that could curb the impacts of air pollution on public health [27].

Since mobility is a multifaceted concept with social, economic, environmental, and political implications [32], we need to situate this term within Ecuador’s socio-economic, political, and historical context to be able to understand not only the impacts of mobility restrictions on the environment but also on the social system. The protests that followed the announcement of economic reforms in October 2019 to deal with the economic crisis in Ecuador brought the capital city of Quito to a standstill with the imposition of a state of emergency and a general curfew for the whole population. The 12-day protests that followed are an example of how economic decisions can further fragment a society already weakened by historical structural inequalities [33] and lead to social unrest, protests, and violence that can paralyze entire cities and affect the movement of goods and services with detrimental impacts to the local and national economies. Months later, the COVID-19 pandemic hit Ecuador particularly hard and contributed to the further worsening of socio-economic conditions with the imposition of extended lockdowns. By April and early May 2020, Ecuador had become one of the significant COVID-19 epicenters in South America due to the high incidence of cases and increased mortality compared to other countries in the region [34]. Here, we analyze the impacts of this type of social unrest on air quality in one of South America’s largest and most populous metropolitan areas in the Andean region.

3. Materials and Methods

To investigate the impacts of social protests and COVID-19 lockdowns on air quality, we evaluated the changes in the average median values of two trace gases, NO₂ and O₃, before and after the major social upheaval events in October 2019 and April 2020. This evaluation relied on remotely sensed estimates of both air parameters, which are readily available through public on-line platforms and because of NO₂’s and O₃’s sensitivity to short-term and sudden changes in human activities. Although other parameters such as particular matter PM₁₀ or PM_{2.5} have an important influence on air quality, the use of satellite observations to accurately estimate near-surface PM mass concentrations remains

challenging because of the relatively poor understanding of the intrinsic relationship between PM and aerosols [35].

We examined changes in the concentrations of these pollutants based on remote sensing data obtained from the Google Earth Engine (GEE) platform, previously validated using ground data from the air quality stations from REMMAQ. We hypothesize that average median pollutant concentrations significantly changed before and after the social protests and the COVID-19 lockdown. We used a paired-sample *t*-test approach at both the 0.05 and 0.001 significance levels to compare the average median estimates for the periods *T*₁ (before the social protests—September 2019); *T*₂ (after the social protests—November 2019); *T*_{1*} (before the imposition COVID-19 lockdown and quarantine measures—March 2020); and *T*_{2*} (after the implementation of lockdown restrictions and generalized quarantines—May 2020). In addition, we also compared the average median values before and after the events for the whole period *T*₁ – *T*_{2*} comprising the two events. Paired-sample *t*-tests have been used to evaluate the spatial and temporal variability of urban air quality [36], indoor and outdoor air quality, the effects of air pollution and perceptions toward air pollution [37], trace gas variation [38], and other dimensions of atmospheric change. We define the general model as follows:

$$t = \frac{a}{SEa}, \quad (1)$$

where *t* is the test statistic, *a* is the difference of group median averages (i.e., difference between average median concentration estimates before and after the social upheaval event) during the following periods: (1) *T*₁ – *T*₂; (2) *T*_{1*} – *T*_{2*}; and (3) *T*₁ – *T*_{2*}. *SE* is the standard error of difference *a*. We obtained average median concentrations from the Tropospheric Monitoring Instrument (TROPOMI) on board the European Copernicus Sentinel-5 Precursor (S5P), previously validated using REMMAQ data collected at eight different stations distributed across the city during the same periods [39]. After validation, we used S5P data from the centroids of randomly selected sub-city district units or parishes (*N* = 30 from a total of 65) using the ArcGIS Pro V3.2 as a geographic information system (GIS) framework. All statistical analyses were performed in SPSS V29.

To facilitate the interpretation of the statistical results, we created the geovisualizations of S5P monthly median concentration estimates for the following periods: (1) September, October, and November 2019; and (2) February, March, April, and May 2020. We cross-checked these visualizations with population density estimates (people/km²) at the parish level to differentiate trends within the borders of Quito's Metropolitan District. We derived population density estimates using the latest data (year 2022) from the Ecuadorian National Census Institute (INEC, 2022) (<https://www.censoecuator.gob.ec/resultados-censo/>, accessed on 1 May 2024). We classified parishes by population density using a mean-standard deviation scheme, summarized the concentrations by class, and created line graphs to visualize temporal trends and compare patterns. All geovisualizations were generated in the software ArcGIS Pro V3.2, with the data extracted from the EE, pandas, and matplotlib library on the Python framework, based in Google Colab.

3.1. The TROPOMI S5P Dataset

S5P is a relatively new satellite mission managed by the European Space Agency (ESA) and launched in October 2017. Its primary purpose is to monitor atmospheric conditions with high spatio-temporal resolution and to be used in air quality, ozone, and ultra-violet (UV) radiation assessments and climate studies. TROPOMI has a native spatial resolution of 5.5 km × 3.5 km and a daily temporal resolution. Its spectral range includes the ultraviolet, shortwave infrared (SWIR), and infrared (IR) bands. The predominant algorithms that retrieve O₃ and NO₂ data from these spectral bands include GODFIT for O₃ offline products and the DOMINO-2 model for NO₂. TROPOMI measures the global Earth radiance by monitoring the 2.3 μm range of SWIR. TROPOMI products can be accessed through the Copernicus hub or other geospatial cloud-based platforms such as GEE. GEE provides significant computational resources and an extensive remote-sensing data catalog [40]. We used two TROPOMI products available in GEE offline (O₃ and NO₂) resampled at a spatial

resolution of 1 km. The TROPOMI O₃ and NO₂ concentration parameters, in this order, are defined as (1) the total atmospheric column of O₃ between the surface and the top of the atmosphere, computed with the GODfit model, and (2) the total vertical column of NO₂ measured as the ratio of the slant column density of NO₂ and the total air mass factor. S5P data are measured in mol/m².

3.2. S5P and REEMAQ Stations Correlations

Remotely sensed data have some limitations associated with internal and external interferences that could affect their quality. O₃ and NO₂ estimates may also include biases due to the vertical variability of concentrations. One of the alternatives to ensure that the remote sensing data represent near-surface conditions is to verify that they correlate with in situ data. Thus, we used REMMAQ network data for this purpose. REMMAQ consists of eight air quality stations that measure O₃ and NO₂ hourly in µg/m³. These stations are distributed across the city (Figure 1), and their data are available at the Quito Environmental Secretary's website (<http://aireambiente.quito.gob.ec/>, accessed on 1 May 2023). In this study, we calculated monthly median estimates based on daily pollutant concentration values between 2018 and 2021 (Table 1).

Table 1. Statistical values of air pollutant parameters.

Parameter (Unit)—Source	N	Mean	Median	Std. Dev.	Min	Max
NO ₂ (µg/m ³)—REMMAQ	222	11.987455	10.855000	6.391611	1.390000	30.080000
NO ₂ (mol/m ²)—S5P	222	0.000050	0.000049	0.000009	0.000035	0.000096
O ₃ (µg/m ³)—REMMAQ	221	50.510452	49.510000	10.497901	29.770000	80.160000
O ₃ (mol/m ²)—S5P	222	0.114695	0.114584	0.003601	0.107391	0.122577

We constructed our remotely sensed concentrations dataset by extracting S5P data for each area around the REMMAQ stations. Then, we compared the satellite estimates with near-surface data obtained from air quality stations using Pearson correlation (*r*) analysis, after testing for normality without considering the variation within the vertical column in the atmosphere. We computed Pearson correlation values for each station and air pollutant to determine the proportion of the variance in the satellite data that the station data could explain. This procedure allowed us to ensure that satellite data accurately represented ground conditions. In addition, this procedure allowed us to explore the potential of using S5P data in air quality assessments in other regions that do not have a network of air quality monitoring stations, extending the applicability of our findings to areas beyond the immediate studied sties.

4. Results

4.1. Correlation between S5P Data and In Situ Observations

We supported our analysis of S5P data through Pearson correlation tests, comparing the median concentrations observed by REMMAQ stations and S5P during the same periods. In the case of NO₂, the highest Pearson correlation values were obtained at the Guamani, Belisario, and Los Chillos stations ($0.55 \leq r \leq 0.78$) (Figure 2). In the case of O₃, correlation values were close to 0.6 at most stations (Figure 3), with the highest *r* values at the Camal, Carapungo, and Cotocollao stations ($0.63 \leq r \leq 0.74$).

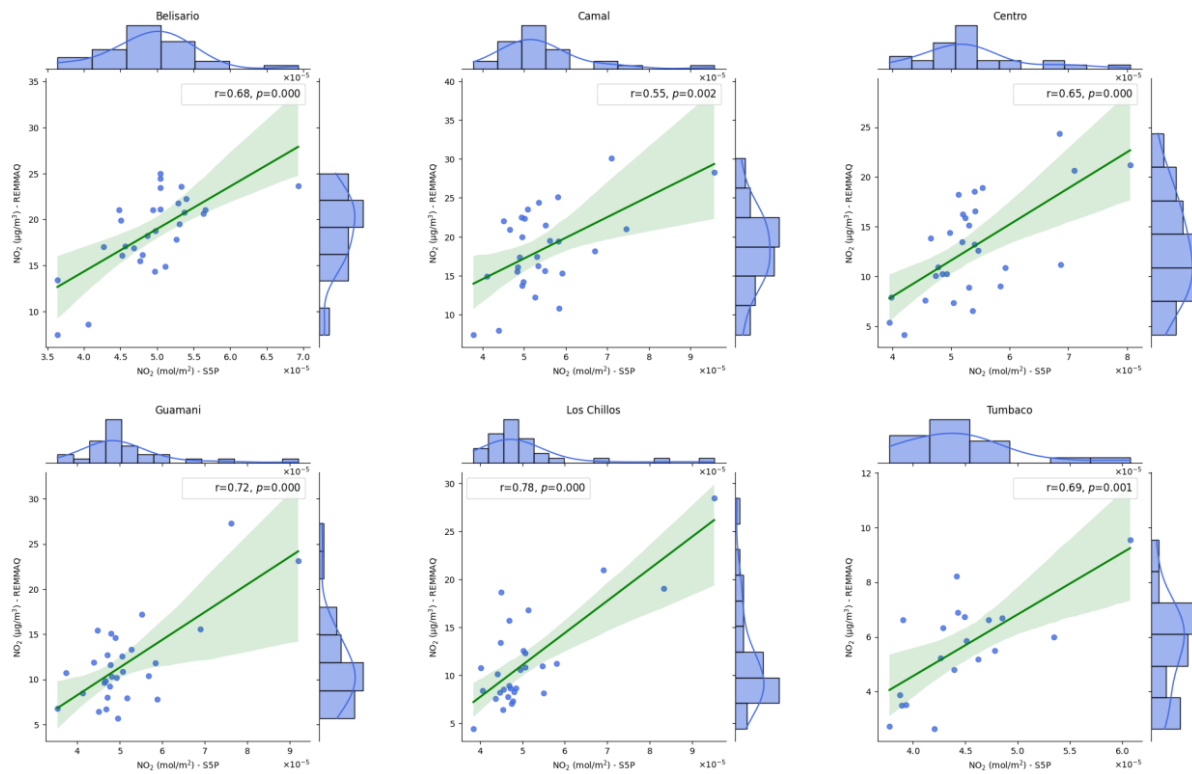


Figure 2. Pearson correlation evaluation of NO₂ monthly median estimates measured by S5P (in mol/m²) and REEMAQ (in µg/m³) per station.

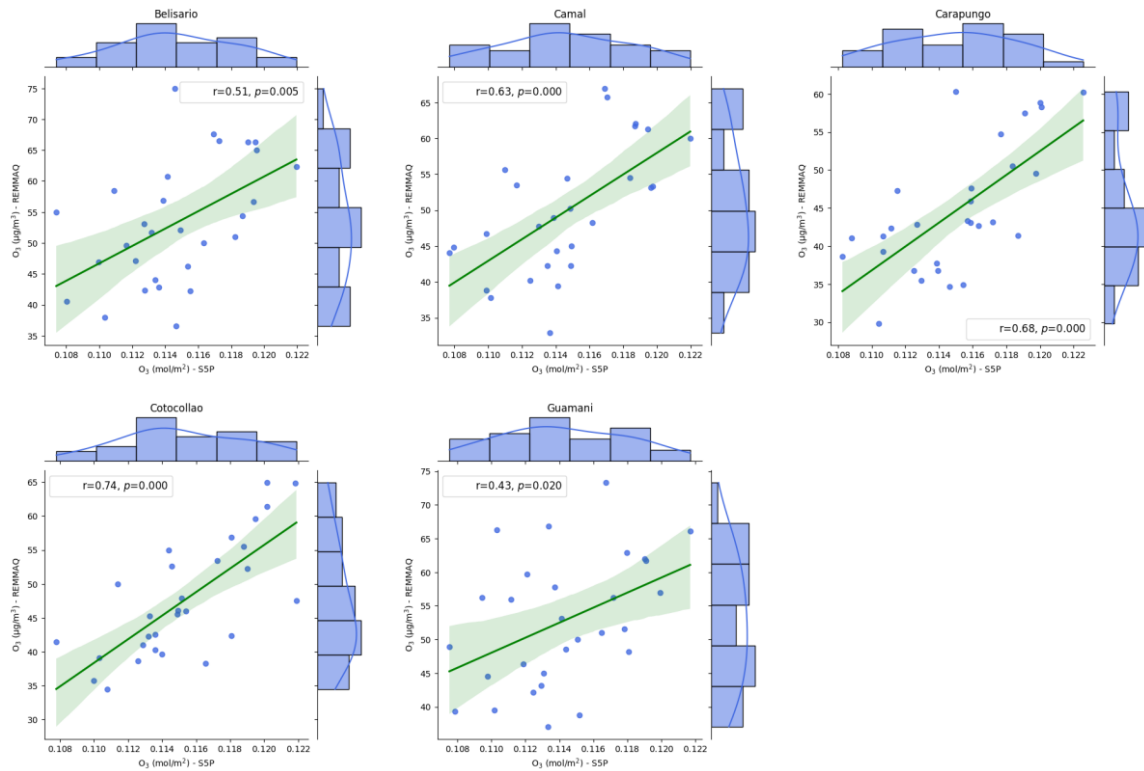


Figure 3. Pearson correlation evaluation of O₃ monthly median estimates measured by S5P (in mol/m²) and REEMAQ (in µg/m³) per station. Bar graphs on the top and side of the scatterplots show the shape of the data distributions.

Figure 2 shows a significant positive correlation between the monthly median NO₂ estimates measured by the S5P satellite and the REEMAQ ground-based measurements for all the stations analyzed. Correlation coefficients vary between 0.55 (Camal) and 0.78 (Los Chillos), indicating that the relationship between these two datasets is consistent, although with variations in strength, being moderate at some stations and very strong at others. The *p*-values of less than 0.05 at all stations reinforce the statistical significance of these correlations. These findings suggest that satellite NO₂ measurements can be a valuable complementary tool to ground-based monitoring networks, helping to improve the accuracy and coverage of air quality monitoring.

Figure 3 shows a significant positive correlation between the monthly median O₃ estimates measured by the S5P satellite and the REMMAQ ground-based measurements. The correlation coefficients vary between 0.43 (Guamani) and 0.74 (Cotocollao), indicating that the relationship between these two datasets is consistent, although with variations in strength, which are moderate at some stations and very strong at others. The *p*-values of less than 0.05 at all stations reinforce the statistical significance of these correlations.

These findings are relevant to air quality monitoring as they demonstrate that O₃ measurements made by S5P can effectively complement ground-based REMMAQ measurements. The ability to obtain accurate O₃ data from the satellite provides a valuable tool for improving the spatial and temporal coverage of air quality monitoring, especially in areas where ground-based infrastructure is limited.

4.2. T-Test Evaluations

Results of the paired *t*-tests showed statistically significant differences during the comparison periods $T1 - T2$, $T1^* - T2^*$, and $T1 - T2^*$ (Table 2) for the two trace gases, which provide possible evidence that the social unrest events likely impacted atmospheric conditions in Quito, as per the evaluation of the remote sensing data. However, the results of this evaluation also show unexpected results regarding the direction of the changes. As anticipated, O₃ experienced significant decreases in their concentrations during the periods $T1 - T2$ (O₃ = −5.51%) and $T1^* - T2^*$ (O₃ = −3.16%). Nevertheless, NO₂ levels significantly increased between $T1^*$ and $T2^*$. This was confirmed by an additional paired *t*-test comparison (Table 2) between February (about one month before the initial restrictions) and March 2020.

Table 2. Results of the paired *t*-test evaluations of average median O₃ and NO₂ estimates based on S5P data.

Period	Trace Gas	Month, Year	Mean (mol/m ²)	Var	Pearson Corr.	Mean Diff.	t Stat	<i>p</i> -Value	Change Direction	Percent Change	
T1	O ₃	Sep 2019	0.115887	0.000000	0.22	−0.006380	59.39	0.000	++	−	−5.51%
T2		Nov 2019	0.109507	0.000000	-	-	-	-	-	-	-
T1*		Mar 2020	0.112569	0.000000	0.52	−0.003555	43.59	0.000	++	−	−3.16%
T2*		May 2020	0.109013	0.000000	-	-	-	-	-	-	-
T1	NO ₂	Sep 2019	0.000043	0.000000	0.56	0.000007	−5.96	0.000	++	+	15.15%
T2		Nov 2019	0.000050	0.000000	-	-	-	-	-	-	-
T1*		Mar 2020	0.000038	0.000000	0.59	0.000004	−8.17	0.000	++	+	9.72%
T2*		May 2020	0.000042	0.000000	-	-	-	-	-	-	-
T1	O ₃	Sep 2019	0.115887	0.000000	0.34	−0.006874	69.11	0.000	++	−	−5.93%
T2*		May 2020	0.109013	0.000000	-	-	-	-	-	-	-
T1	NO ₂	Sep 2019	0.000043	0.000000	0.53	−0.000002	2.64	0.013	+	−	−3.62%
T2*		May 2020	0.000042	0.000000	-	-	-	-	-	-	-

N = 30; Df = 29; t critical = 2.045. ++ Significant at a 0.001 level; + Significant at a 0.05 level.

($T1^*$), just for NO₂, showed a significant decrease in this gas (mean diff = −0.000005, *p* < 0.001, percent change = −10.74%). When comparing NO₂ at a longer temporal scale (between September 2019 and March 2020), we observed a significant overall reduction in the period covering both events (−3.62%) between September 2019 ($T1$) and May 2020 ($T2^*$). In contrast, O₃ decreased by 7.34% and 5.93% respectively.

4.3. Incidence of Social Upheaval Events on Air Quality

We evaluated the concentration of our target trace gases using S5P data at the ground station locations. O_3 levels peaked in September and started to decline in October 2019 during the social protests. The dataset shows a gradual increase following this decrease in O_3 from January to March 2020. During the lockdown in April 2020, air quality improved, as shown by declining O_3 levels across most REMMAQ stations (Figure 4).

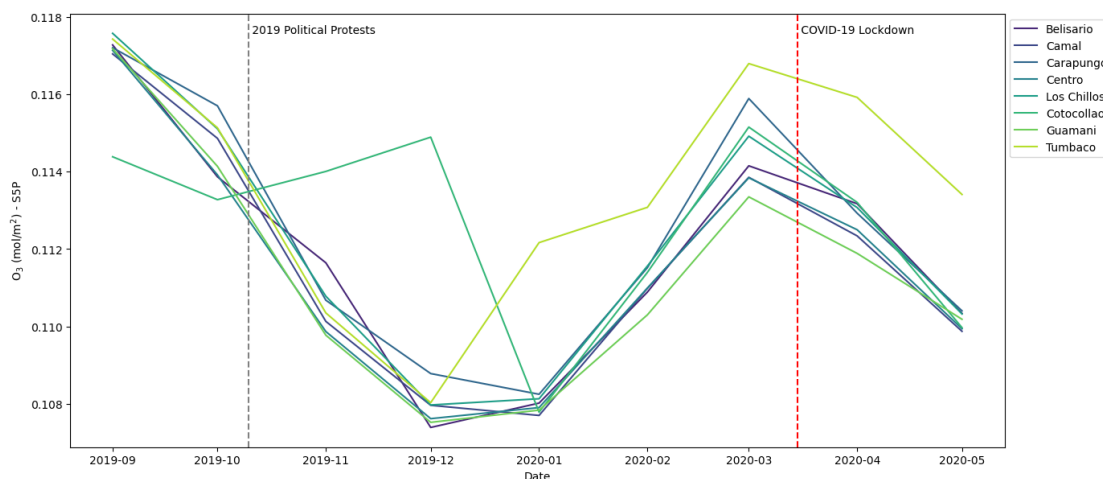


Figure 4. Temporal variation of O_3 measurements derived from S5P data between September 2019 and May 2020. The vertical black line indicates the start of the 2019 political protests, and the red line indicates the beginning of the COVID-19 lockdown.

The NO_2 dataset showed an increase before and after the October 2019 event, followed by a decreasing trend starting February 2020, even before the imposition of COVID-19 restrictions toward the end of March (Figure 5). Results from our correlation analysis confirm this association (Figure 3). Specifically, the Belisario, Camal, Centro, and Tumbaco stations exhibited similar trends for both datasets, while the Cotocollao station showed a different pattern.

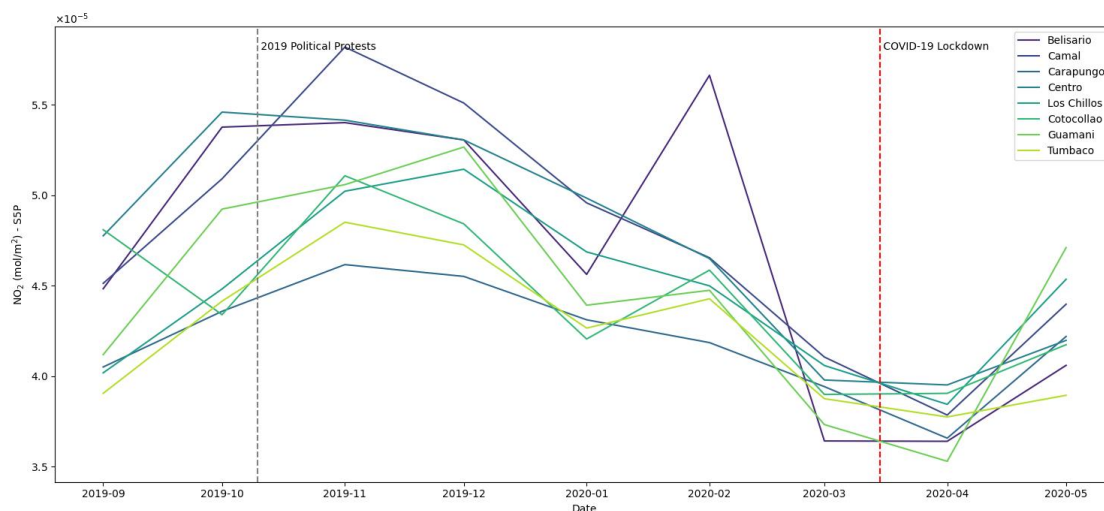


Figure 5. Temporal variation in NO_2 measurements derived from S5P data between September 2019 and May 2020. The vertical black line indicates the start of the 2019 political protests, and the red line indicates the beginning of the COVID-19 lockdown.

4.4. Mapping and Comparing Air Quality Using Remotely Sensed Data

The spatial distribution of pollutant concentrations across the study area during September 2019 and November 2019, and during February 2020 and May 2020 is highly variable. Our geovisualizations illustrate distinctive temporal patterns in NO₂ (Figure 6) and O₃ concentrations (Figure 7), likely linked to population density variation at the sub-city district level.

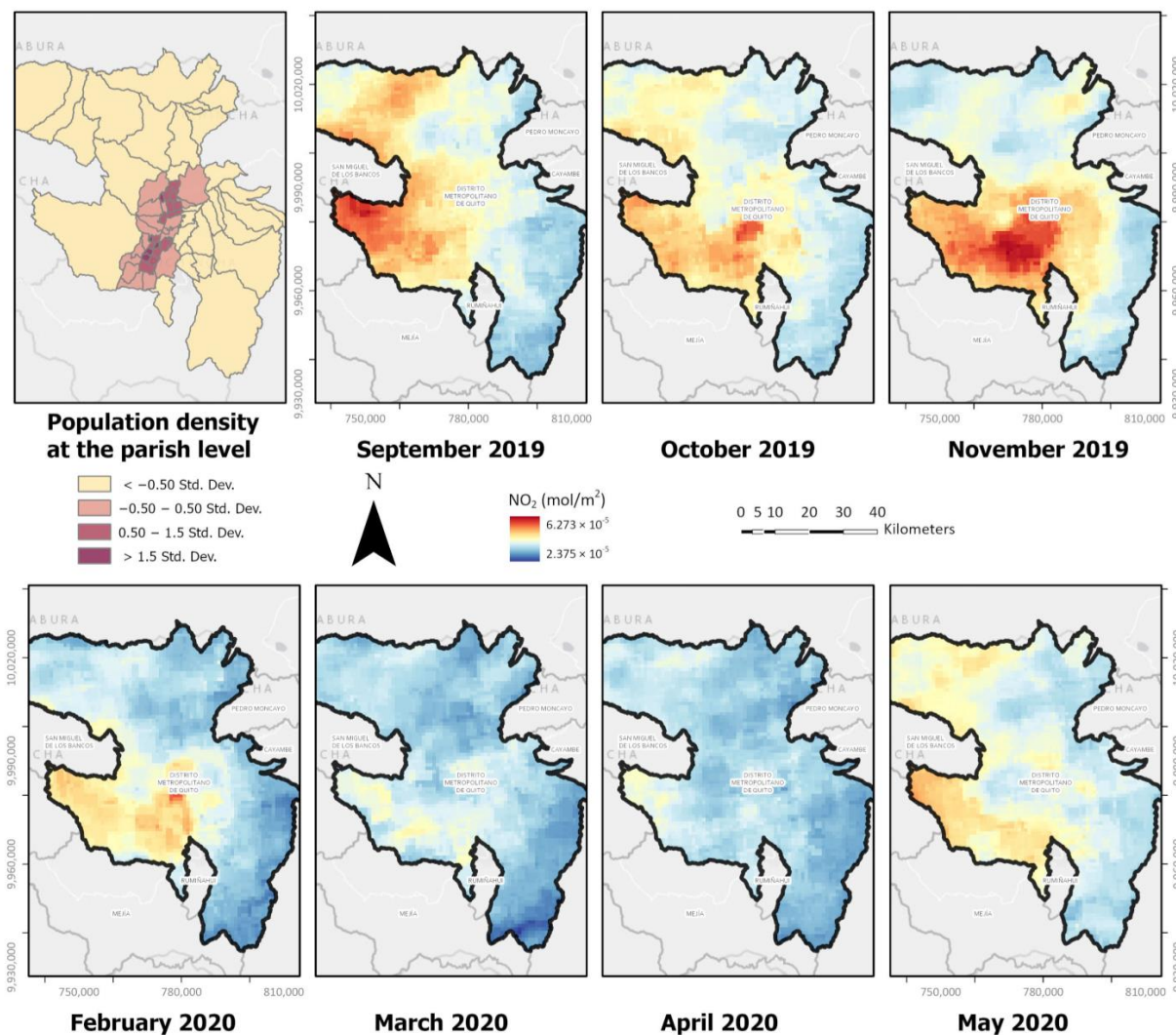


Figure 6. NO₂ geovisualizations generated using population density at the parish level in Quito and TROPOMI S5P data obtained from Google Earth Engine during the following time periods: (1) September–November 2019 and (2) February–May 2020.

During the first period, NO₂ concentrations were the highest in the most densely populated parishes (Quito’s urban center), as shown by the dark red areas in Figure 6. By November 2019, elevated NO₂ levels had spread into suburban regions, accompanied by the dispersion and significant decrease in O₃ concentrations (Figure 7). This shift highlights the changing pollution dynamics over time.

Figures 6 and 8 offer essential comparisons of NO₂ concentrations on specific dates (i.e., October 2019, February 2020, and April 2020), and across the whole analysis period. From October to November 2019 (public protest period) NO₂ concentrations were higher in parishes with population densities above 1.5 standard deviations above the mean (i.e., zones with higher protest activity). In contrast, areas with population density less than -0.5 standard deviation below the mean (i.e., zones with less protest activity) exhibited

more stable levels over time. Additionally, during the COVID lockdown (March–April 2020), overall NO_2 concentrations in the city were lower, with less variation between parishes of differing population densities. This suggests that changes in human activity levels during protests and lockdowns substantially impact pollutant concentrations.

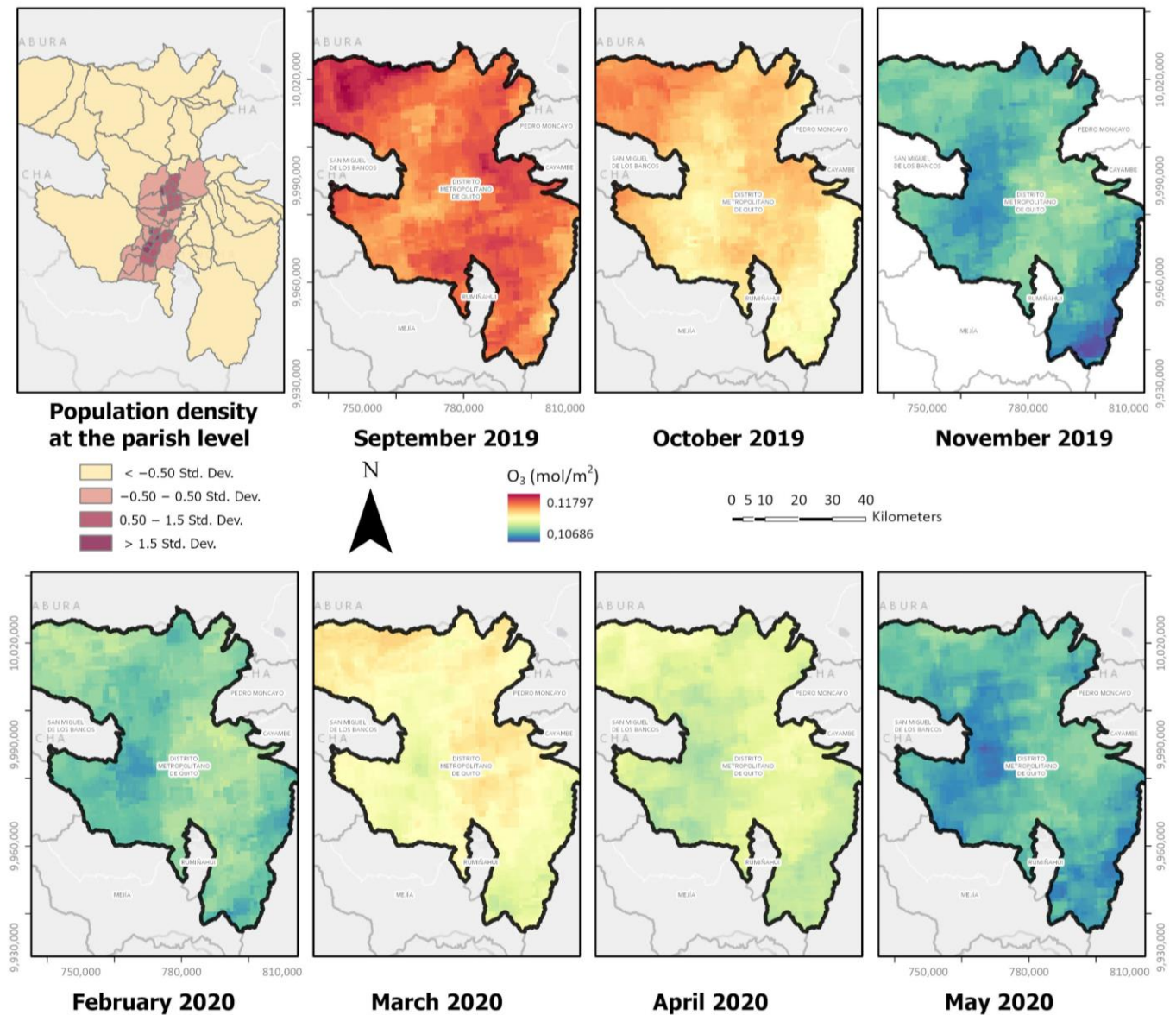


Figure 7. O_3 geovisualizations generated using population density at the parish level in Quito and TROPOMI S5P data obtained from Google Earth Engine for the following time periods: (1) September–November 2019 and (2) February–May 2020.

In contrast, O_3 concentrations (Figure 7) showed higher levels in February 2020 than in 2019, particularly in more densely populated areas with minimal protest activity. This suggests a correlation between pollutant concentration levels and human activity. Figure 9 further highlights these trends, showing a decrease in O_3 concentrations during the civil protests and an increase during the COVID-19 lockdown. This change is evident across all four population density categories, illustrating a consistent pattern.

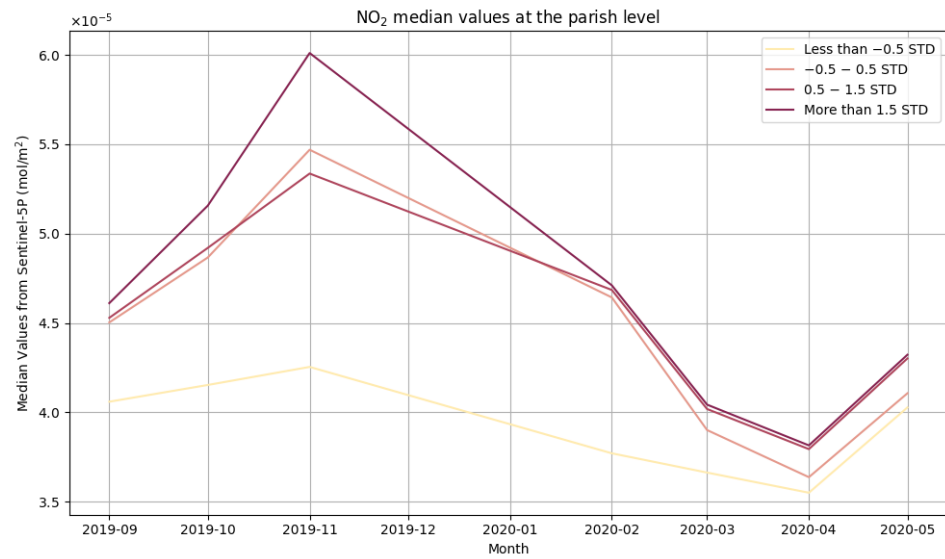


Figure 8. NO₂ median value concentration at the parish level in Quito. Each line represents the density of the population according to categories based on one standard deviation.

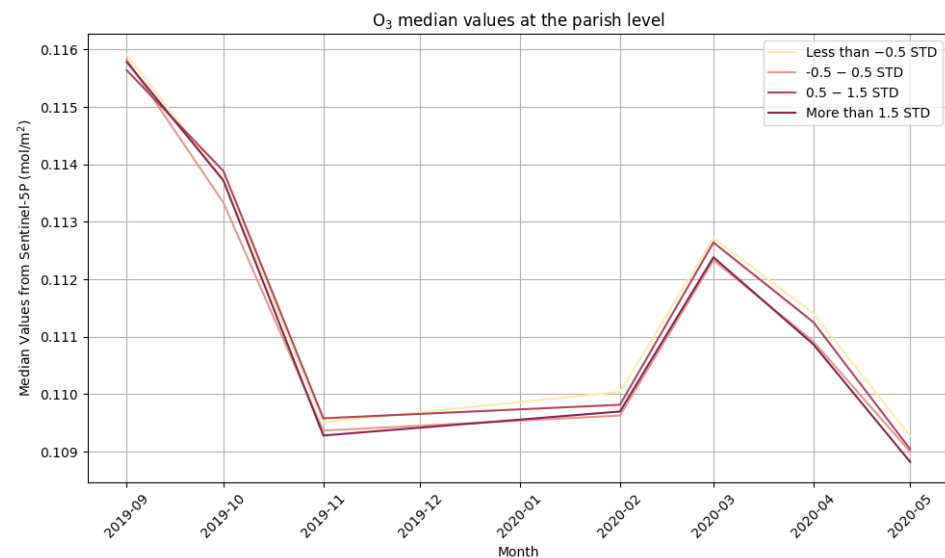


Figure 9. O₃ median value concentration at the parish level in Quito. Each line represents the density of the population according to categories based on one standard deviation.

5. Discussion

In this study, we evaluated the impact of social unrest events on air quality as depicted by changes in concentration levels of two important trace gases: O₃ and NO₂. For this purpose, we relied on the information derived from S5P to analyze and visualize changes in average median concentrations over time. We first cross-checked the satellite data with estimates collected by air monitoring stations to ensure that the remotely sensed information reliably captured and represented near-surface conditions during the analysis periods. We found consistent trends between the data collected by REMMAQ and S5P for the two gases, as shown by the statistical significance of the correlation tests. Nevertheless, a temporal lag of about one month exists between the values obtained by the satellite and the monitoring stations. This lag is probably due to local atmospheric conditions that could have affected how the ground sensors and satellite registered the near surface values and within the vertical column of the gases respectively [41]. In addition, near-surface air quality conditions could also be affected by the geographic location of monitoring stations, local atmospheric conditions (particularly wind patterns), and the amount of road traffic.

Although a more effective way of validating S5P could have included the use of statistical methods that rely on common deviation measurements (e.g., root mean square error, mean standard error, etc.), these techniques require all datasets to be in the same measurement units and scale, and although the transformation from $\mu\text{g}/\text{m}_3$ to mol/m_2 is possible, it is not recommended since precise gas column height values are required but not readily available for all locations [42]. For this reason, we relied on a correlation analysis to depict the association between information gathered by S5P and ground stations. Our Pearson correlation analysis results showed that the correlation coefficients (r values) were high for O_3 and NO_2 in some stations, which is consistent with the results reported in previous studies for other regions [43,44]. This finding highlights that S5P data usually lead to a more accurate depiction of O_3 and NO_2 levels [45]. We should note that NO_2 and O_3 are closely linked because, in addition to climate and geographic factors, the O_3 formation depends on NO_2 concentrations [46,47]. This co-dependence may explain why these two gases also show similar r values. The correlation values for NO_2 ranged from 0.55 to 0.78 and from 0.63 to 0.74 for O_3 at the air monitoring stations. The correlations between satellite-based data and ground measurements provide confidence that the satellite data can be used to study the impacts of these events. Although the differences in NO_2 and O_3 concentration levels between satellite and ground measurements were not fully evaluated, our results suggest that air quality models could be developed that include social events as another driving factor. By combining remote sensing with meteorological, social, and other relevant environmental information, we could greatly improve our understanding of air quality at local levels. While remote sensing has limitations, it provides useful initial information that could be used to better understand the changes caused by short-term events like social protests and lockdowns.

The statistical analysis corroborated most of our assumptions regarding the significance of changes in air quality months before and after the social upheaval events in Quito, which is also consistent with the findings by Zambrano-Monserrate and Ruano (2020) at a temporal scale of one year that the levels of NO_2 were the highest during the social protests in October 2019, despite decreased vehicular traffic compared to February and March 2020. This increase in NO_2 levels can be attributed to the significant burning of waste and other materials such as tires and plastics with gasoline and other oil-derived products during the protests, resulting in considerable air pollution in the city. Local citizens employ these common tactics during social protests to block roads and disrupt traffic. Additionally, data from ground stations at Camal and Belisario indicated very high NO_2 concentration estimates that exceeded or nearly reached the upper limit recommended by the World Health Organization [48,49]. NO_2 concentrations nearing this limit pose a health risk. Conversely, during the COVID-19 lockdown period, we observed higher concentrations of O_3 in relation to NO_2 at the same stations, indicating that an increase in O_3 leads to a decrease in NO_2 . O_3 levels also notably decreased between September and November 2019, suggesting an overall improvement in air quality. This reduction is likely associated with a substantial decrease in motorized traffic and lowered use of fossil fuels. In addition, O_3 is formed through photochemical reactions involving NO_2 and sunlight, where solar radiation and the photolysis of NO_2 contribute to increased O_3 and reduced NO_2 levels [50].

In general, the pandemic-related events in Ecuador resulted in a significant decrease in human activities between February 2020 and May 2020, which in turn led to a reduction in air pollutant concentrations and improved air quality, as shown by the t -test comparisons of average median concentrations of the two analyzed gases before and after the events. This finding is consistent with previous air quality studies that relied on REM-MAQ data only [51]. Specifically, we rejected the null hypothesis of equal average median concentrations of paired groups. We confirmed that air quality before and after the social upheaval events statistically changed during our analysis periods $T1-T2$, $T1^*-T2^*$, and $T1-T2^*$. However, while our study found that O_3 concentrations decreased during these periods, NO_2 concentrations increased. Since mobility restrictions started towards the

end of March, we also compared average median NO₂ concentration changes between February and March 2020 and found a statistically significant decrease for this gas. This finding suggests that motorized traffic had already experienced a considerable decline even before the generalized lockdown restrictions were implemented at the end of March 2020, probably when the number of positive cases increased exponentially in the country, which had already impacted mobility. For example, S5P data show significant reductions in NO₂ levels at the Belisario and Guamani station locations of 35% and 18%, respectively, in March compared to the levels observed in February 2020. The average reduction in NO₂ concentration across all station locations was 18% based on S5P data alone between February and March 2020.

March 2020 shows the lowest average median NO₂ values for the study period (September 2019–May 2020). Although NO₂ concentration levels remained low during March and part of April (when stricter lockdown measures were implemented), these increased again by the end of April and May 2020, as depicted by the statistically significant increase in average median concentrations between March and May 2020. Although further research is needed to be able to identify the exact reasons why such a significant increase occurred despite the application of lockdown measures, one could hypothesize that the change could have been associated with (1) geographic conditions, including solar activity, wind conditions, humidity, and other environmental factors; and (2) increases in commercial traffic and public transportation (e.g., trucks, buses) and other industrial operations within the city limits that did not entirely stop despite the mobility restriction measures, and in some cases, probably increased to satisfy the demand for goods and services of the population under lockdown.

Based on the statistical results, we created geovisualizations of NO₂ and O₃ concentrations using S5P data. These spatial depictions are useful for visualizing overall changes over time and detecting spatial variations in concentration estimates across the metropolitan district. We observed that NO₂ concentrations were particularly high in areas with significantly high protest activity (October–November 2019) and higher population densities. This indicates a possible correlation between the population density and NO₂ concentrations. Interestingly, during the COVID-19 lockdown period (March–April 2020), NO₂ levels decreased across the city, and O₃ concentrations exhibited less variation, as shown by a more uniform color pattern. This uniformity may be related to local weather conditions, such as wind and sunlight, which could have affected the distribution of the pollutants [52].

Finally, through the geovisualization of gas concentrations, we demonstrated the advantages of using a cloud-based platform such as GEE to obtain a detailed and geolocated understanding of air quality variation in a large urban conglomerate [53]. Furthermore, by interpreting remote sensing data and analyzing social conditions like population density, we provided new insights into particular social behaviors and their impact on short-term atmospheric patterns.

6. Conclusions

This study evaluated air quality changes during social upheaval events using S5P data, previously validated with ground station data from REMMAQ. Our findings indicate an acceptable correlation between near-surface air quality data from REMMAQ stations and satellite data, particularly for O₃ and NO₂. This information was summarized in statistical estimates, graphs, and geovisualizations, which helped us to comprehensively characterize Quito's air quality conditions during the two social upheaval events in 2019 and 2020. Our study suggests that social upheaval events generate short-term positive and negative externalities in the environment or a simultaneous bi-directional response depending on the gas type. We found that, for example, social protests, usually accompanied by increased human activity and environmental disturbances, led to increased air pollution levels throughout the city's urban core, as reflected by increases in NO₂ levels probably associated with the burning of waste. However, O₃ concentrations decreased during the same period,

probably linked to reduced vehicular traffic, sunlight, and other weather conditions. The COVID-19 lockdown improved air quality, as depicted by the decreased air pollutant concentrations of the two gases. However, the timing of the responses varies depending on the type of gas. While O₃ decreased between March and May 2020, NO₂ increased during the same period. NO₂ estimates, on the other hand, decreased between February and March 2020, before the lockdown restrictions were in place. These findings suggest that drawing general conclusions about the overall impacts of social upheaval events on air quality and atmospheric conditions may not be feasible. Air quality assessments require studying trace gases separately to better understand their individual impacts, sources, interactions, and effects on the environment in the long term. This detailed knowledge is necessary for developing targeted strategies to mitigate air pollution and maintain acceptable air quality standards across the range of gases.

Understanding air quality is paramount for evaluating a region's overall quality of life, as environmental changes are intricately linked to human well-being, including effective responses to numerous pollution concerns. The vulnerability of urban populations to air pollution is notably high due to the pervasive generation of air pollutants through daily routine activities linked to fossil-fuel-based transportation and industrial operations near or within city limits [54]. Poor air quality conditions, for instance, significantly impact the respiratory health of a region's inhabitants. Therefore, improved air quality monitoring strategies are pivotal in ensuring the well-being of urban dwellers in times of accelerated environmental change and pressing socio-economic challenges [55]. Consequently, the significance of remote sensing has increased in recent years not only because it can be used to track atmospheric changes during relatively short time periods which could help assess air quality almost real-time but also because remote sensing is a cost-effective alternative for developing countries that lack the resources to implement costly air monitoring networks [56–58]. Spatial and temporal air quality monitoring methods, like those presented in this study, provide an alternative for collecting and analyzing data that could be eventually integrated into effective controls and interventions based on readily and near-real-time observations. This technology can provide tangible evidence of humans' impacts on the Earth's system, which could be used to generate policies to curb local-to-global environmental crises [59].

Author Contributions: Conceptualization, C.I.A. and D.V.; methodology, C.I.A., S.L. and D.V.; software, C.I.A. and D.V.; validation, C.I.A., S.L. and D.V.; formal analysis, C.I.A. and S.L.; investigation, C.I.A., S.L., D.V. and D.G.; resources, C.I.A. and S.L.; data curation, C.I.A. and D.V.; writing—original draft preparation, D.V., D.G. and C.I.A.; writing—review and editing, D.V., D.G. and C.I.A.; visualization, D.V.; supervision, C.I.A. and S.L.; project administration, C.I.A.; funding acquisition, C.I.A. All authors have read and agreed to the published version of the manuscript.

Funding: This research received no external funding.

Data Availability Statement: The original contributions presented in the study are included in the article, further inquiries can be directed to the corresponding author.

Acknowledgments: We thank the research team for all the help and support provided while developing this work.

Conflicts of Interest: The authors declare no conflicts of interest.

References

1. Diffenbaugh, N.; Field, C.; Appel, E.; Azevedo, I.; Baldocchi, D.; Burke, M.; Burney, J.; Ciaia, P.; Davis, S.; Fiore, A.M.; et al. The COVID-19 Lockdowns: A Window into the Earth System. *Nat. Rev. Earth Environ.* **2020**, *1*, 470–481. [[CrossRef](#)]
2. Luginaah, I.; Fung, K.; Gorey, K.; Shahedul, K. The Impact of 9/11 on the Association of Ambient Air Pollutions with Daily Respiratory Hospital Admissions in a Canada-US Border City, Windsor, Ontario. *Int. J. Environ. Stud.* **2006**, *63*, 501–5014. [[CrossRef](#)] [[PubMed](#)]
3. Beck, M.J.; Hensher, D.A. Insights into the Impact of COVID-19 on Household Travel and Activities in Australia—The Early Days under Restrictions. *Transp. Policy* **2020**, *96*, 76–93. [[CrossRef](#)] [[PubMed](#)]

4. Du, J.; Rakha, H.; Filali, F.; Eldardiry, H. COVID-19 Pandemic Impacts on Traffic System Delay, Fuel Consumption and Emissions. *Int. J. Transp. Sci. Technol.* **2021**, *10*, 184–196. [[CrossRef](#)]
5. Nižetić, S. Impact of Coronavirus (COVID-19) Pandemic on Air Transport Mobility, Energy, and Environment: A Case Study. *Int. J. Energy Res.* **2020**, *44*, 10953–10961. [[CrossRef](#)]
6. Kinver, M. Then and Now: Pandemic Clears the Air. BBC 2021. Available online: <https://www.bbc.com/news/science-environment-57149747> (accessed on 29 October 2023).
7. Franzosi, R. One Hundred Years of Strike Statistics: Methodological and Theoretical Issues in Quantitative Strike Research. *ILR Rev.* **1989**, *42*, 348–362. [[CrossRef](#)]
8. Meinardi, S.; Nissenson, P.; Barletta, B.; Dabdub, D.; Rowland, S.; Blake, D. Influence of the Public Transportation System on the Air Quality of a Major Urban Center. A Case Study: Milan, Italy. *Atmos. Environ.* **2008**, *42*, 7915–7923. [[CrossRef](#)]
9. Zalakeviciute, R.; Alexandrino, K.; Mejia, D.; Bastidas, M.G.; Oleas, N.H.; Gabela, D.; Chau, P.N.; Bonilla-Bedoya, S.; Diaz, V.; Rybarczyk, Y. The Effect of National Protest in Ecuador on PM Pollution. *Sci. Rep.* **2021**, *11*, 17591. [[CrossRef](#)]
10. Cornejo, D.; Rodriguez, F.; Guasumba, A.; Toulkeridis, T. Contrasting Effects of Air Pollution Assessment in Two Areas of the Quito Metropolitan District, Ecuador. *La Granja* **2022**, *36*, 98–112. [[CrossRef](#)]
11. Connolly, R.E.; Yu, Q.; Wang, Z.; Chen, Y.H.; Liu, J.Z.; Collier-Oxandale, A.; Papapostolou, V.; Polidori, A.; Zhu, Y. Long-Term Evaluation of a Low-Cost Air Sensor Network for Monitoring Indoor and Outdoor Air Quality at the Community Scale. *Sci. Total Environ.* **2022**, *807*, 150797. [[CrossRef](#)]
12. Mancero Chicaiza, E.J.; Mancero Chicaiza, E.J. Evaluación de La Calidad Del Aire Durante El Tiempo de Protestas En Ciudades Sudamericanas. *Rev. Geogr. Norte Gd.* **2023**, *2023*, 159–176. [[CrossRef](#)]
13. Bauernschuster, S.; Hener, T.; Rainer, H. When Labor Disputes Bring Cities to a Standstill: The Impact of Public Transit Strikes on Traffic, Accidents, Air Pollution, and Health. *Am. Econ. J. Econ. Policy* **2017**, *9*, 1–37. [[CrossRef](#)]
14. Bauwens, M.; Stavrakou, T.; Müller, J.F.; De Smedt, I.; Van Roozendaal, M.; Van Der Werf, G.R.; Wiedinmyer, C.; Kaiser, J.W.; Sindelarova, K.; Guenther, A. Nine Years of Global Hydrocarbon Emissions Based on Source Inversion of OMI Formaldehyde Observations. *Atmos. Chem. Phys.* **2016**, *16*, 10133–10158. [[CrossRef](#)]
15. Baldasano, J.M. COVID-19 Lockdown Effects on Air Quality by NO₂ in the Cities of Barcelona and Madrid (Spain). *Sci. Total Environ.* **2020**, *741*, 140353. [[CrossRef](#)] [[PubMed](#)]
16. Huang, G.; Sun, K. Non-Negligible Impacts of Clean Air Regulations on the Reduction of Tropospheric NO₂ over East China during the COVID-19 Pandemic Observed by OMI and TROPOMI. *Sci. Total Environ.* **2020**, *745*, 141023. [[CrossRef](#)]
17. The National Academy of Sciences. *Climate Change Evidence and Causes: Update 2020*; The National Academy of Sciences: Washington, DC, USA, 2020.
18. EPA Basic Information about NO₂ | US EPA. Available online: <https://www.epa.gov/no2-pollution/basic-information-about-no2> (accessed on 29 October 2023).
19. Reddington, C.L.; Conibear, L.; Knote, C.; Silver, B.J.; Li, Y.J.; Chan, C.K.; Arnold, S.R.; Spracklen, D.V. Exploring the Impacts of Anthropogenic Emission Sectors on PM_{2.5} and Human Health in South and East Asia. *Atmos. Chem. Phys.* **2019**, *19*, 11887–11910. [[CrossRef](#)]
20. Khalaf, E.M.; Mohammadi, M.J.; Sulistiyani, S.; Ramírez-Coronel, A.A.; Kiani, F.; Jalil, A.T.; Almulla, A.F.; Asban, P.; Farhadi, M.; Derikondi, M. Effects of Sulfur Dioxide Inhalation on Human Health: A Review. *Rev. Environ. Health* **2022**, *39*, 331–337. [[CrossRef](#)]
21. Zhang, Z.; Zhu, L. A Review on Unmanned Aerial Vehicle Remote Sensing: Platforms, Sensors, Data Processing Methods, and Applications. *Drones* **2023**, *7*, 398. [[CrossRef](#)]
22. Turner, M.C.; Jerrett, M.; Pope, C.A.; Krewski, D.; Gapstur, S.M.; Diver, W.R.; Beckerman, B.S.; Marshall, J.D.; Su, J.; Crouse, D.L.; et al. Long-Term Ozone Exposure and Mortality in a Large Prospective Study. *Am. J. Respir. Crit. Care Med.* **2016**, *193*, 1134–1142. [[CrossRef](#)]
23. Mollocana, J.; Álvarez, C.; Jaramillo, L. Assessment of Fuel Related Data in the Metropolitan District of Quito for Modeling and Simulation of Wildfires, Case Study: Atacazo Hill Wildfire. *La Granja* **2021**, *34*, 45–62.
24. Thies, B.; Bendix, J. Satellite Based Remote Sensing of Weather and Climate: Recent Achievements and Future Perspectives. *Meteorol. Appl.* **2011**, *18*, 262–295. [[CrossRef](#)]
25. Marć, M.; Tobiszewski, M.; Zabiegała, B.; Guardia, M.; Namieśnik, J. Current Air Quality Analytics and Monitoring: A Review. *Anal. Chim. Acta* **2015**, *853*, 116–126. [[CrossRef](#)]
26. Faltynkova, A.; Johnsen, G.; Wagner, M. Hyperspectral Imaging as an Emerging Tool to Analyze Microplastics: A Systematic Review and Recommendations for Future Development. *Microplastics Nanoplastics* **2021**, *1*, 13. [[CrossRef](#)]
27. Alvarez-Mendoza, C.I.; Teodoro, A.; Freitas, A.; Fonseca, J. Spatial Estimation of Chronic Respiratory Diseases Based on Machine Learning Procedures—An Approach Using Remote Sensing Data and Environmental Variables in Quito, Ecuador. *Appl. Geogr.* **2020**, *123*, 102273. [[CrossRef](#)]
28. Álvarez, C. The Use of Remote Sensing in Air Pollution Control and Public Health. In *Socio-Environmental Research in Latin America. The Latin American Studies Book Series*; Springer: Berlin/Heidelberg, Germany, 2023; pp. 139–157. ISBN 978-3-031-22679-3.
29. Jain, S.; Sharma, T. Social and Travel Lockdown Impact Considering Coronavirus Disease (COVID-19) on Air Quality in Megacities of India: Present Benefits, Future Challenges and Way Forward. *Aerosol Air Qual. Res.* **2020**, *20*, 1222–1236. [[CrossRef](#)]
30. Forster, T.; Santini, G. Reinforcing Rural-Urban Linkages Resilient Food Systems. 2015. Available online: <https://openknowledge.fao.org/server/api/core/bitstreams/9ff9bb27-ec9a-49c4-9f7e-81253ee28c9f/content> (accessed on 29 October 2023).

31. Duan, Y.; Ji, T.; Lu, Y.; Wang, S. Environmental Regulations and International Trade: A Quantitative Economic Analysis of World Pollution Emissions. *J. Public Econ.* **2021**, *203*, 104521. [[CrossRef](#)]
32. Díaz, F.; Palacio, M. Inequality and the Socioeconomic Dimensions of Mobility in Protests: The Cases of Quito and Santiago. *Glob. Policy* **2021**, *12*, 78–90. [[CrossRef](#)]
33. Zalakeviciute, R.; Vasquez, R.; Bayas, D.; Buenano, A.; Mejia, D.; Zegarra, R.; Diaz, V.; Lamb, B. Drastic Improvements in Air Quality in Ecuador during the COVID-19 Outbreak. *Aerosol Air Qual. Res.* **2020**, *20*, 1783–1792. [[CrossRef](#)]
34. Alava, J.J.; Guevara, A. A Critical Narrative of Ecuador’s Preparedness and Response to the COVID-19 Pandemic. *Public Health Pract.* **2021**, *2*, 1–3. [[CrossRef](#)]
35. Hoff, R.M.; Christopher, S.A. Remote Sensing of Pariculate Pollution from Space: Have We Reached the Promised Land? *J. Air. Waste Manag. Assoc.* **2009**, *129*, 645–675. [[CrossRef](#)]
36. Chattopadhyay, S.; Gupta, S.; Saha, R.N. Spatial and Temporal Variation of Urban Air Quality: A GIS Approach. *J. Environ. Prot. (Irvine Calif.)* **2010**, *01*, 264–277. [[CrossRef](#)]
37. Wong-Parodi, G.; Dias, M.B.; Taylor, M. Effect of Using an Indoor Air Quality Sensor on Perceptions of and Behaviors toward Air Pollution (Pittsburgh Empowerment Library Study): Online Survey and Interviews. *JMIR mHealth uHealth* **2018**, *6*, e8273. [[CrossRef](#)] [[PubMed](#)]
38. Zambrano, M.; Ruano, M. Has Air Quality Improved in Ecuador during the COVID-19 Pandemic? A Parametric Analysis. *Air Qual. Atmos. Health* **2020**, *13*, 929–938. [[CrossRef](#)]
39. Heue, K.P.; Loyola, D.; Romahn, F.; Zimmer, W.; Chabrilat, S.; Errera, Q.; Ziemke, J.; Kramarova, N. Tropospheric Ozone Retrieval by a Combination of TROPOMI/S5P Measurements with BASCOE Assimilated Data. *Atmos. Meas. Tech.* **2022**, *15*, 5563–5579. [[CrossRef](#)]
40. Gorelick, N.; Hancher, M.; Dixon, M.; Ilyushchenko, S.; Thau, D.; Moore, R. Google Earth Engine: Planetary-Scale Geospatial Analysis for Everyone. *Remote Sens. Environ.* **2017**, *202*, 18–27. [[CrossRef](#)]
41. Grzybowski, P.T.; Markowicz, K.M.; Musiał, J.P. Estimations of the Ground-Level NO₂ Concentrations Based on the Sentinel-5P NO₂ Tropospheric Column Number Density Product. *Remote Sens.* **2023**, *15*, 378. [[CrossRef](#)]
42. UNDP. *COVID-19 Impact on Air Quality in Ukraine and the Republic of Moldova Work Order*; UNDP: New York, NY, USA, 2020.
43. Kelly, J.; Zhao, J.; Xing, J.; Zhang, Y.; Han, S.; Kundhikanjana, W.; Towashiraporn, P.; Stratoulas, D. Interpolation-Based Fusion of Sentinel-5P, SRTM, and Regulatory-Grade Ground Stations Data for Producing Spatially Continuous Maps of PM_{2.5} Concentrations Nationwide over Thailand. *Atmosphere* **2022**, *13*, 161. [[CrossRef](#)]
44. Morillas, C.; Alvarez, S.; Serio, C.; Masiello, G.; Martinez, S. TROPOMI NO₂ Sentinel-5P Data in the Community of Madrid: A Detailed Consistency Analysis with in Situ Surface Observations. *Remote Sens. Appl. Soc. Environ.* **2024**, *33*, 101083. [[CrossRef](#)]
45. Soleimany, A.; Grubliauskas, R.; Šerevičienė, V. Application of Satellite Data and GIS Services for Studying Air Pollutants in Lithuania (Case Study: Kaunas City). *Air Qual. Atmos. Health* **2021**, *14*, 411–429. [[CrossRef](#)]
46. Han, S.; Bian, H.; Feng, Y.; Liu, A.; Li, X.; Zeng, F.; Zhang, X. Analysis of the Relationship between O₃, NO and NO₂ in Tianjin, China. *Aerosol Air Qual. Res.* **2011**, *11*, 128–139. [[CrossRef](#)]
47. Zoran, M.A.; Savastru, R.S.; Savastru, D.M.; Tautan, M.N. Assessing the Relationship between Ground Levels of Ozone (O₃) and Nitrogen Dioxide (NO₂) with Coronavirus (COVID-19) in Milan, Italy. *Sci. Total Environ.* **2020**, *740*, 140005. [[CrossRef](#)] [[PubMed](#)]
48. World Health Organization (WHO). *WHO Global Air Quality Guidelines*; WHO: Geneva, Switzerland, 2021.
49. Targino, A.C.; Harrison, R.M.; Krecl, P.; Glantz, P.; de Lima, C.H.; Beddows, D. Surface Ozone Climatology of South Eastern Brazil and the Impact of Biomass Burning Events. *J. Environ. Manag.* **2019**, *252*, 109645. [[CrossRef](#)] [[PubMed](#)]
50. Ravina, M.; Caramitti, G.; Panepinto, D.; Zanetti, M. Air Quality and Photochemical Reactions: Analysis of NO_x and NO₂ Concentrations in the Urban Area of Turin, Italy. *Air Qual. Atmos. Health* **2022**, *15*, 541. [[CrossRef](#)]
51. Atiaga, O.; Guerrero, F.; Páez, F.; Castro, R.; Collahuazo, E.; Nunes, L.M.; Grijalva, M.; Grijalva, I.; Otero, X.L. Assessment of Variations in Air Quality in Cities of Ecuador in Relation to the Lockdown Due to the COVID-19 Pandemic. *Heliyon* **2023**, *9*, e17033. [[CrossRef](#)] [[PubMed](#)]
52. Berman, J.D.; Ebisu, K. Changes in U.S. Air Pollution during the COVID-19 Pandemic. *Sci. Total Environ.* **2020**, *739*, 139864. [[CrossRef](#)]
53. Alvarez-Mendoza, C.I.; Lopez, S.; Vasquez, D. Monitoring Air Quality Using Remote Sensing Based on a Google Earth Engine Application in Countries with Limited Air Quality Data and Control Policies: A Case Study in Ecuador. *Remote Sens. Technol. Appl. Urban Environ. VIII* **2023**, *12735*, 80–85. [[CrossRef](#)]
54. Kumar, P.; Singh, A.B.; Arora, T.; Singh, S.; Singh, R. Critical Review on Emerging Health Effects Associated with the Indoor Air Quality and Its Sustainable Management. *Sci. Total Environ.* **2023**, *872*, 162163. [[CrossRef](#)]
55. Tran, H.M.; Tsai, F.J.; Lee, Y.L.; Chang, J.H.; Chang, L.T.; Chang, T.Y.; Chung, K.F.; Kuo, H.P.; Lee, K.Y.; Chuang, K.J.; et al. The Impact of Air Pollution on Respiratory Diseases in an Era of Climate Change: A Review of the Current Evidence. *Sci. Total Environ.* **2023**, *898*, 166340. [[CrossRef](#)] [[PubMed](#)]
56. Alvarez, C.; Teodoro, A.; Torres, N.; Vivanco, V. Assessment of Remote Sensing Data to Model PM₁₀ Estimation in Cities with a Low Number of Air Quality Stations: A Case of Study in Quito, Ecuador. *Environments* **2019**, *6*, 85. [[CrossRef](#)]
57. Lane, T.P.; King, A.D.; Perkins-Kirkpatrick, S.E.; Pitman, A.J.; Alexander, L.V.; Arblaster, J.M.; Bindoff, N.L.; Bishop, C.H.; Black, M.T.; Bradstock, R.A.; et al. Attribution of Extreme Events to Climate Change in the Australian Region—A Review. *Weather Clim. Extrem.* **2023**, *42*, 100622. [[CrossRef](#)]

-
58. Xu, R.; Yu, P.; Liu, Y.; Chen, G.; Yang, Z.; Zhang, Y.; Wu, Y.; Beggs, P.J.; Zhang, Y.; Boocock, J.; et al. Climate Change, Environmental Extremes, and Human Health in Australia: Challenges, Adaptation Strategies, and Policy Gaps. *Lancet Reg. Health-West. Pacific* **2023**, *40*, 100936. [[CrossRef](#)] [[PubMed](#)]
 59. Jones, G.S.; Stott, P.A.; Christidis, N. Attribution of Observed Historical Near-Surface Temperature Variations to Anthropogenic and Natural Causes Using CMIP5 Simulations. *J. Geophys. Res. Atmos.* **2013**, *118*, 4001–4024. [[CrossRef](#)]

Disclaimer/Publisher’s Note: The statements, opinions and data contained in all publications are solely those of the individual author(s) and contributor(s) and not of MDPI and/or the editor(s). MDPI and/or the editor(s) disclaim responsibility for any injury to people or property resulting from any ideas, methods, instructions or products referred to in the content.